IVYSPRING INTERNATIONAL PUBLISHER

Theranostics

2018; 8(2): 358-368. doi: 10.7150/thno.21099

Research Paper

Parametric optimization of electric field strength for cancer electrochemotherapy on a chip-based model

Deyao Zhao[1], Mengxi Wu[2, 3], Dong Huang[2], Zicai Liang[1]✉, Zewen Wei[4]✉ and Zhihong Li[2]✉

1. Institute of Molecular Medicine, Peking University, Beijing 100871, China;
2. National Key Laboratory of Science and Technology on Micro/Nano Fabrication, Institute of Microelectronics, Peking University, Beijing 100871, China;
3. Department of Engineering Science and Mechanics, The Pennsylvania State University, State College, PA 16801, USA;
4. National Center for Nanoscience and Technology, Beijing 100190, China.

✉ Corresponding authors: Zhihong Li (zhhli@ime.pku.edu.cn, Fax 86-10-62751789), Zicai Liang (liangz@pku.edu.cn, Fax +86-10-62769862), or Zewen Wei (weizw@nanoctr.cn, Fax 86-10-82545752).

Received: 2017.05.19; Accepted: 2017.10.08; Published: 2018.01.01

Abstract

Electrochemotherapy (ECT), as one of the very few available treatments for cutaneous and subcutaneous tumors when surgery and radiotherapy are no longer available, requires applying a proper electric field to the tumor to realize electroporation-mediated cytotoxic drug delivery. It is impossible to exhaust all possible electrical parameters on patients to realize the optimal tradeoff between tumor suppression and adverse effects. To address this issue, this study provides a feasible solution by developing a four-leaf micro-electrode chip (F-MEC) in which the electric field was specially designed by linear distribution to cover all possible electric field strengths for ECT.

Methods: We developed a F-MEC that provides a linearly varied electric field and a capacity for *in situ* observation of cell status. By culturing tumor cells on the F-MEC surface and *in situ* monitoring the cell responses to ECT drugs, the optimal electric field strength for any given cell type could be rapidly and accurately calculated in a few, or even only one, simple assay.

Results: Using this chip, we monitored MCF-7 and A315 cell responses to ECT and determined the optimum ECT voltage. More importantly, we successfully verified that the *in vitro* determined voltage coincided with the optimal value for *in vivo* ECT in mice.

Conclusion: In this proof-of-concept study, the *in vivo* tumor suppression assays proved that the optimal parameters acquired from *in vitro* F-MEC assay could be used for *in vivo* ECT.

Key words: Electroporation, Electrochemotherapy, Drug Delivery.

Introduction

Electrochemotherapy (ECT) is currently an established method for the local treatment of cutaneous and subcutaneous tumors [1-4] if surgery and radiotherapy are no longer available [5, 6]. ECT combines administration of non-permeant or poorly-permeant chemotherapeutic drugs with application of *in vivo* cell electroporation to facilitate drug delivery into tumor cells [7-13]. Since 1988, when ECT was first proved *in vitro* [14], many clinical studies had demonstrated its safety and effectiveness [1, 2, 15]. As a result, ECT has gradually become an accepted clinical method. A standard operating procedure (SOP) for ECT was issued in 2006, as a milestone for the technology [16]. This undoubtedly increased the usage of ECT in clinics, especially in the European Union [17]. In 2012, more than 3,000 patients were treated with ECT in the European Union [18].

To perform ECT, cytotoxic drugs are first injected, either intravenously or intramuscularly, into patients to obtain an adequate drug concentration in tumor tissue [3]. Then, a sufficiently high electric field is applied to the tumor [19-22]. Thus, the tumor cells exposed to the electric field are electroplated to

uptake the cytotoxic drugs [21, 23]. Once the electric field is removed, the permeable cell membrane reseals accordingly [24, 25]. The drugs accumulate in the cell interior to eventually kill the tumor cells and suppress tumor growth [26]. In ECT process, the drug type and electrical parameters are two dominant factors affecting the therapeutic effects of ECT. Currently, bleomycin has outperformed other candidate drugs and has become predominant in ECT, benefiting from the higher potentiation of its cytotoxicity [26-34]. Another prospective drug, cisplatin, is still under clinical evaluation [21, 23, 35]. However, compared with selecting a proper drug from very limited options, deciding the optimal electrical parameters from a wide variety of combinations is far more challenging. Because of the cell heterogeneity, different cancers may demand entirely different electrical parameters to achieve the optimum therapeutic effects. Thus it is quite likely that the voltage needs to be varied, sometimes dramatically, while electroporating different kinds of cells. In the SOP of ECT [16], there are recommend voltages for each kind of electrode, such as 960 V for a pair of parallel plate-electrodes with 8 mm spacing or 400 V for needle-like electrodes with 3 mm spacing [27]. The corresponding electric field strength approximately ranges from 1000 V/cm to 1350 V/cm. The reason of appointing a fixed high voltage for each kind of electrode, ignoring the differences among diverse cancer types, is to ensure killing of the cancer cells and simplify the diagnosis/treatment procedures [36]. Following the SOP, fixed voltage has been used in the majority of clinical practices, in which varying degrees of adverse reactions have been reported, such as pain, bleeding, electrically burnt skin and uncontrollable muscle contraction [27, 37]. Some of these adverse effects might be alleviated by reducing the voltage according to cancer type or individual diversities, since the fixed high voltage may be excessive for some patients. In fact, it was considered necessary to add cancer-type-dependent voltages into the decision tree while compiling the new modified SOP [27].

It is impossible to exhaust all combinations of electrical parameters on patients. It was demonstrated that *in vitro* optimized electrical parameters could be used for *in vivo* ECT [28-33]. Further clinical study proved the *in vitro* optimization of electrical parameters was a useful guidance for the treatment of patients [30]. Various studies explored *in vitro* optimization of electrical parameters for ECT by employing commercial apparatus, such as electroporation cuvettes [30] and parallel plate-electrodes [33]. Using these commercial devices, parameter optimization is still a time-consuming and costly process, in which plenty of parallel assays should be performed to exhaust all possible parameters. This is obviously not practical for large-scale clinical applications. Customized micro-devices have also been used to investigate behavior of tumor cells [38, 39], especially their responses to ECT [40, 41]. However, the lack of *in vivo* verification limits the clinical usage of existing micro-devices on ECT.

To address these issues, this study explored a different strategy. For a specific cancer type, we intended to use only one assay to acquire the optimum ECT voltage. We developed a simple four-leaf micro-electrode chip (F-MEC) that provides a linearly varied electric field and a capacity for *in situ* observation of cell status. Using this chip, we monitored cell responses to ECT and determined the optimum ECT voltage. More importantly, we successfully verified that the *in vitro* determined voltage coincided with the optimal value for *in vivo* ECT in mice.

Experimental section

Materials, cells and animals

Therapeutic bleomycin hydrochloride (Takasaki Plant, Nippon Kayaku Co. Ltd, Japan) was used in ECT assays. The bleomycin hydrochloride powder was dissolved in PBS buffer with a concentration of 15 mg/mL. A modified hypo-osmolar electroporation buffer (25 mM KCl, 0.3 mM KH_2PO_4, 0.85 mM K_2HPO_4, 36 mM myo-inositol) was used for ECT assays. Before performing ECT, the bleomycin solution was diluted to 150 μg/mL by electroporation buffer.

For *in vitro* ECT assays, MCF-7 (human breast adenocarcinoma cell) and A375 (human melanoma cells) cells were used. Both kinds of cells were grown in Dulbecco's modified Eagle's medium (DMEM) that was supplemented with 10% fetal bovine serum (Sigma-Aldrich), 100 units/mL penicillin and 100 μg/mL streptomycin (Gibco). Cells were incubated at 37°C in 5% CO_2 humidified atmosphere. All cells were seeded in culture dish (Corning) 2–3 days prior to the experiments.

For *in vivo* ECT assays, female BALB/c nude mice (18-22 g) were purchased from Vital River Laboratories (Beijing, China). For tumor inoculation, 7.5×10^6 MCF-7 cells were injected subcutaneously into the right axillary fossa of the BALB/c nude mice. Animals were maintained in Peking University Laboratory Animal Center, which is an AAALAC-accredited and specific pathogen free (SPF) experimental animal facility. All of the experimental animals in our study were treated in accordance with

protocols approved by the Institutional Animal Care and Use Committee of Peking University.

ECT protocols

For *in vitro* ECT assays, cultured cells were harvested by trypsin treatment and resuspended to a density of about 4×10^5 cells/mL in cell culture medium. For each F-MEC, 8×10^4 cells (200 μL) were added and incubated for at least 4 h for cells to adhere on the chip surface, then 1 mL DMEM was added per F-MEC and incubated overnight. Before performing ECT, all media was removed. Cells were washed with electroporation buffer three times and 10 μL bleomycin-electroporation buffer solution (150 μg/mL) was dropped on F-MEC. Electric stimulation was applied by ECM-830 stimulator (BTX, USA). After electroporation, 1 mL of cell culture medium was added onto each F-MEC immediately for *in situ* cell culture.

For *in vivo* ECT assays, the tumors were grown to ~300 mm^3 before experiments. In the ECT experiment, all mice were anesthetized by intraperitoneal (i.p.) injection with pentobarbital sodium (50 mg/kg). 20 μL (1 mg/mL) hyaluronidase was injected into 4 positions within the tumor tissue by changing the needle head direction. After 15 min, 100 μL bleomycin-electroporation buffer solution (150 μg/mL) was injected into the tumor in the same area using the same method. Then the tumor was covered by 2 parallel electroporation plates and 10 electric pulses, provided by ECM-830 stimulator (BTX, USA), were applied for electrical stimulation.

Determination of ECT efficiency and tumor suppression

To determine *in vitro* ECT efficiency, 48 h after ECT, cells were stained with Hoechst (bisBenzimide H 33342 trihydrochloride, Sigma-Aldrich), and F-MEC was fluorescently imaged. Cells were enumerated by analyzing fluorescence images using a NIH recommended software ImageJ. To determine tumor suppression, ECT was performed on each mouse every three days. The tumor sizes were monitored for 17 days. The relative tumor volume was calculated by normalizing the mean tumor volume of post-treatment mice to the corresponding mean tumor volume before treatments.

Results

The four-leaf micro-electrode chip (F-MEC)

Figure 1A shows the four-leaf micro-electrode chip (F-MEC), which consists of a glass substrate and four leaf-shaped electrodes. As shown in the enlarged Figure 1B, we positioned several signs with diverse patterns in each electrode to assist visually determining the electric field strength. As shown in Figure 1C, the interior edges of the electrodes were designed in conformity with the hyperbolic equation (1).

$$y = \pm 1.9/x \qquad (1)$$

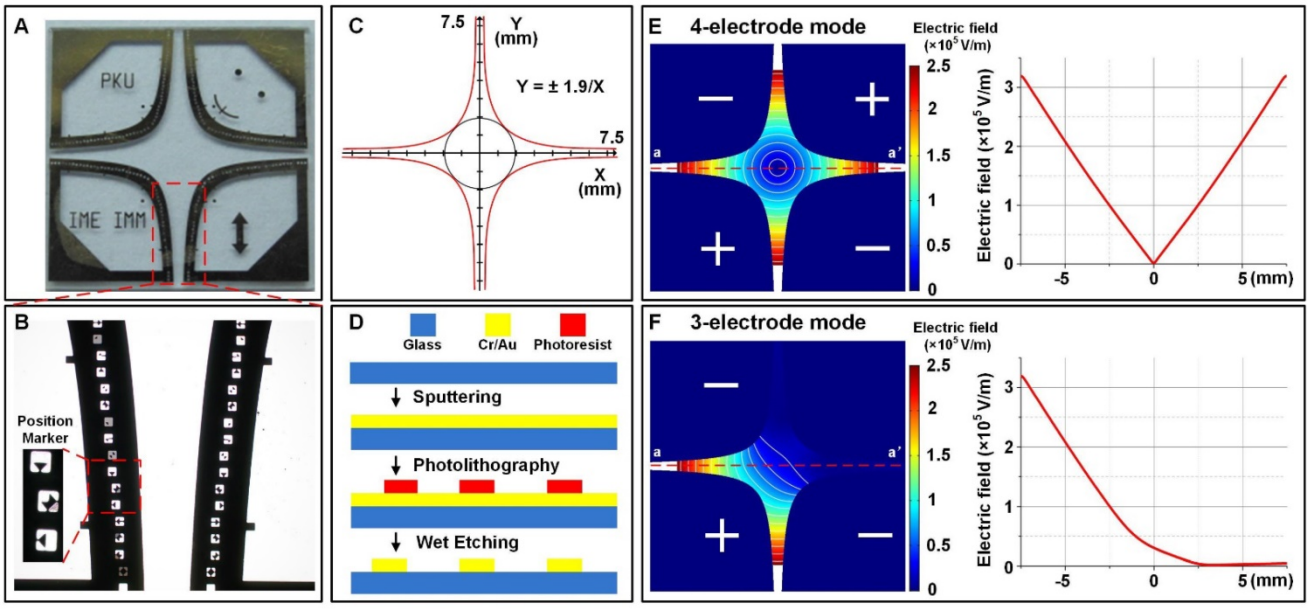

Figure 1. The four-leaf micro-electrode chip (F-MEC) (A) Photo of four-leaf micro-electrode chip (F-MEC). (B) The position markers fabricated in the electrodes. (C) The four-leaf electrodes are designed in conformity with a hyperbolic equation (D) the fabrication process of F-MEC. The electric field strength distributions of four-electrode (E) and three-electrode (F) modes were simulated by FEA software Comsol Ver.3.5a.

Figure 1D shows the simple fabrication process of F-MEC. A 4 inch Pyrex® 7740 glass wafer (500 μm thick) was used as substrate because of its high transparency, which benefits the *in situ* observation of cells. A gold layer (300 nm thick) was sputtered on the glass wafer and patterned by wet etching to form the electrodes. To enhance adhesion, there was a chrome layer (30 nm thick) between gold and glass. Finally, the wafer was diced to 15 mm x 15 mm quadrates. Both glass and gold exhibited good bio-compatibility, benefiting cell culture on the chip surface.

The chip has two electrical stimulation modes. The first one is four-electrode mode, as shown in Figure 1E, where the opposing two electrodes are connected to the same polarity. The electric field intensity at the central point is zero because of the geometrical symmetry. In the central area and the four apertures between the electrodes, the electric field strength is annularly distributed. For instance, along the axis aa', if 150 V was applied, the electric field strength decreased from 3.2×10^5 V/m to 0 V/m, then bounced back to 3.2×10^5 V/m. The gradient of this variation was 4.27×10^7 V/m^2. The second is three-electrode mode (Figure 1F), in which one of the four electrodes is disconnected. Thus, only two apertures are applied with linearly varied electric field, while the other two exhibit no electric field, serving as an on-chip control area. In both stimulation modes, the electric field was designed to vary linearly, thus providing convenience in rapid investigation and visual determination of electric field strength.

In vitro parametric optimization of ECT

ECT is based on cell electroporation. Firstly, using HEK-293A cells and pEGFP-C3 DNA plasmids, we demonstrated the capability of F-MEC to rapidly determine the optimal cell electroporation parameters (Supplementary Figure S1). Briefly, we cultured cells on the surface of F-MEC, and then applied a voltage on F-MEC to generate a linearly varied electric field in which all cells were exposed. By *in situ* observing all electroporated cells, we found some cells were dead because of the excessive electric field strength, some cells remained alive but not GFP-expressed because the electric field was insufficient, and the rest of the cells showed both high viability and efficient GFP expression. Since the positions of all cells directly indicated the electric field strength applied on them, by determine the position of well-electroporated cells, we could easily obtain the corresponding optimal electric field strength.

We then investigated the electroporation-assisted chemotherapeutic drug uptake, which is the key process of ECT. We used MCF-7 cells, a breast cancer cell line, and bleomycin, a predominant ECT drug, to evaluate the effect of electroporation-assisted bleomycin uptake. Four-electrode mode was used on F-MEC. First, we applied only electric field on MCF-7 cells, without adding bleomycin, to evaluate electroporation-induced cell death, excluding its interference in further assays. As shown in Figure 2A, almost all cells remained on the chip surface (stained by Hoechst), even in the periphery area of the chip, where the electric field strength was up to 7×10^4 V/m. The results demonstrated that irreversible cell membrane damage, which would induce immediate cell detachment, was negligible while the electric field strength was lower than 7×10^4 V/m. We then explored the joint effect of bleomycin and electric field on MCF-7 cells to evaluate the electroporation-assisted bleomycin uptake. As shown in Figure 2B, a 100 V voltage was applied for cell viability observation. Cells remained in the central area, where the electric field was weak. From inner area to outer area, the electric field strength was linearly increased. When the electric field strength was higher than 3×10^4 V/m, cells began to detach; when the electric field strength was greater than 4×10^4 V/m, most cells were detached. The results demonstrated that the boundary between cell existence and detachment was between 3×10^4 and 4×10^4 V/m. To verify this range, we decreased the voltage from 100 V to 80 V (Figure 2C). As the electric field weakened, the cell existence area correspondingly expanded. Despite the variation in the cell death/survival pattern, the transition from cell existence to cell detachment still occurred between 3×10^4 to 4×10^4 V/m. Apart from monitoring cell existence by Hoechst staining, we also employed Calcein AM and Propidium Iodide (PI) to fluorescently indicate cell survival and death, respectively (Supplementary Figure S2). The results revealed that in the scenario of our chip-based study, almost all remaining cells were alive while most of the dead cells detached from the chip surface. Therefore, the Hoechst staining images revealed that the effective electric field for ECT was between 3×10^4 and 4×10^4 V/m. These results demonstrate that a proper electric field facilitates chemotherapeutic drug uptake, and we can rapidly determine the effective range of the electric field by *in situ* observing cell status.

While performing ECT, to maximize chemotherapeutic drug uptake and corresponding tumor inhibition, the electric field should be stronger than a threshold. We investigated this threshold using F-MEC under three-electrode mode. Differed from four-electrode mode, the three-electrode mode left one electrode disconnected (for example, the upper right one in Figure 3), generating approximate zero

electric field areas on chip. Cells located in these areas were considered as control group to differentiate the effect of bleomycin alone from the joint effect of bleomycin and electric field. We firstly applied 100 V on the chip. As shown in Figure 3A, the boundary districting cell life and death was located between 3×10^4 and 4×10^4 V/m contours. Most cells survived in the zero electric field area, indicating bleomycin treatment without electric enhancement had limited inhibition to MCF-7 cells. When we increased the voltage from 100 V to 150 V (Figure 3B), the electric field distribution varied, and the cell survival area shrunk accordingly. However, the boundary between cell life and death was still located between 3×10^4 and 4×10^4 V/m contours. These results demonstrated one merit of the F-MEC: we don't need to specify an optimal experimental F-MEC voltage for each kind of cells. The electric field threshold that differentiates cell life and death could be easily determined by one-time *in-situ* observation of cell status. We also monitored the cell apoptosis process by Annexin staining (Annexin V-FITC Apoptosis Detection Kit, Sigma-Aldrich) (Supplementary Figure S3) to ensure that the dominant effect causing cell death was ECT.

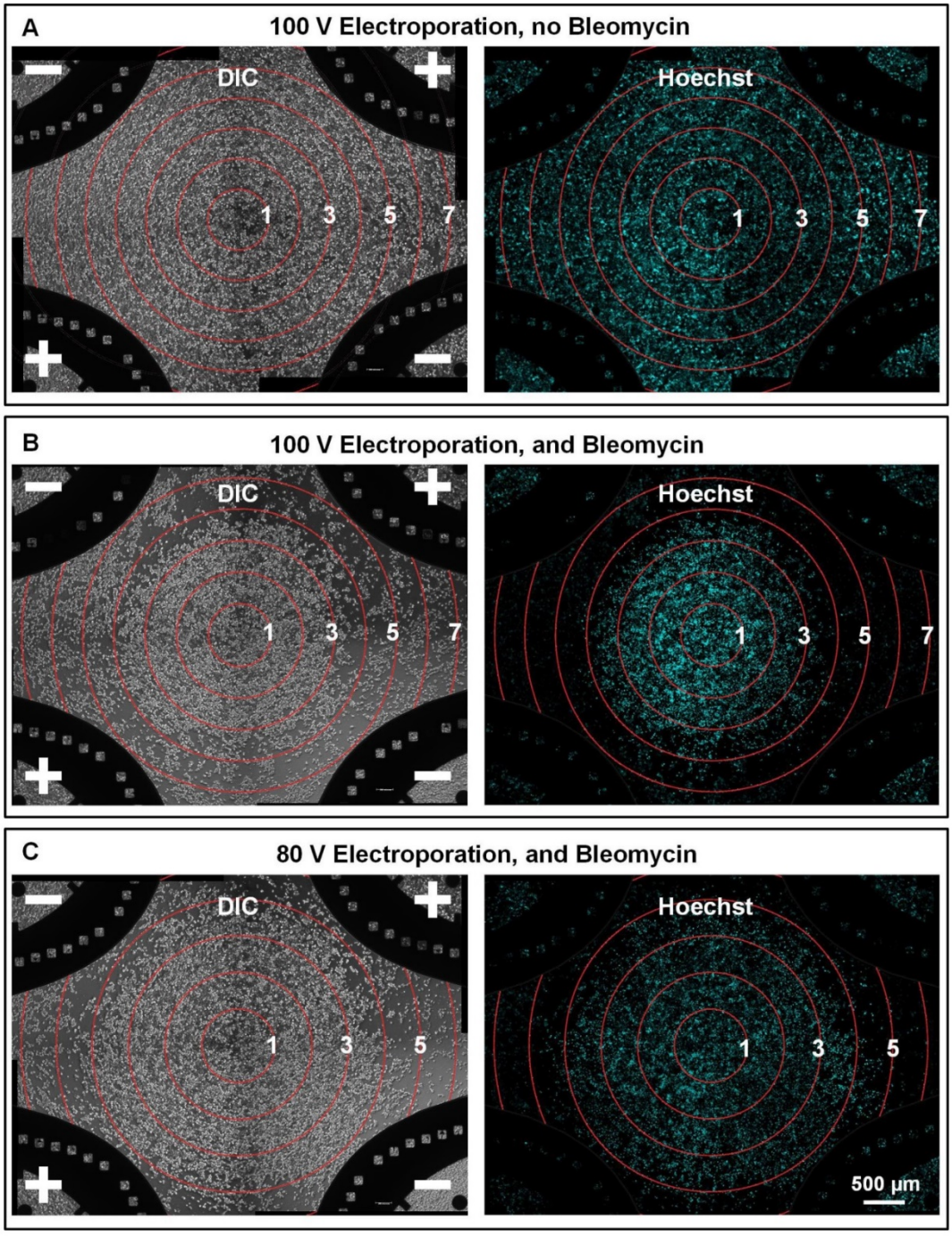

Figure 2. In situ monitoring the bleomycin responses of MCF-7 cells on F-MEC under four-electrode stimulation mode Bright field images (left) and fluorescence images (right) of Hoechst stained MCF-7 cells 48 h after performing *in vitro* ECT with four-electrode stimulation mode. The conditions are: (A) 100 V voltage, no bleomycin; (B) 100 V and 150 μg/mL bleomycin (C) 80 V and 150 μg/mL bleomycin. For (A), (B) and (C), 8 square electrical pulses (100 μs pulse duration and 1 s interval) were applied. In each image, the electric field contours are marked by red rings and the Arabic numerals on the curves represent the contour values (unit: $\times10^4$ V/m).

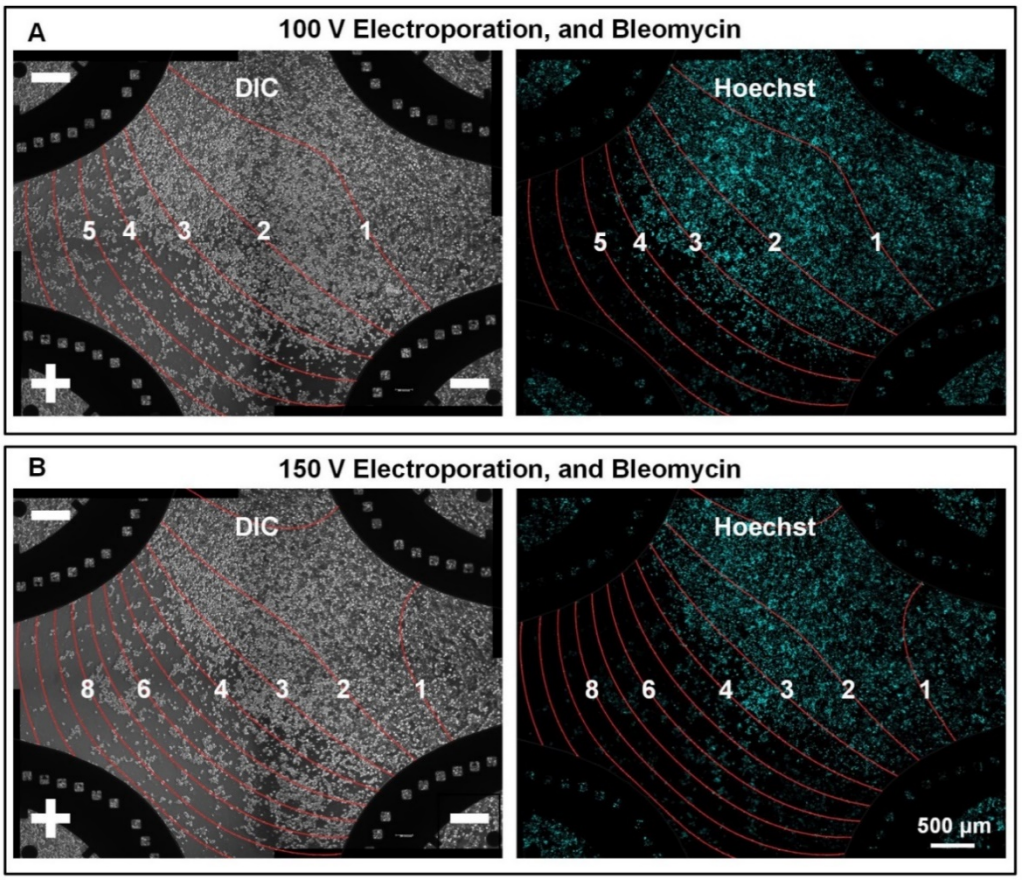

Figure 3. In situ monitoring the bleomycin responses of MCF-7 cells on F-MEC under three-electrode stimulation mode Bright field images (left) and fluorescence images (right) of Hoechst stained MCF-7 cells 48 h after performing *in vitro* ECT with three-electrode stimulation mode. The upper right electrode was disconnected from the electric stimulator. The conditions are: (A) 100 V and 150 μg/mL bleomycin; (B) 150 V and 150 μg/mL bleomycin. For both (A) and (B), 8 square electrical pulses (100 μs pulse duration and 1 s interval) were applied. In each image, the electric field contours are marked by red curves and the Arabic numerals on the curves represent the contour values (unit: $\times 10^4$ V/m).

In many cases, providing a numerical range of suitable electric field strength, such as from 3×10^4 to 4×10^4 V/m, is enough for guiding ECT. However, further analyzing the bleomycin responses of cells to acquire more accurate optimal electric field strength is a better option for performing precise ECT. The electric field on F-MEC is linearly distributed. Therefore, by using markers located in electrodes (square grids in Figure 4A), it is easy to plot electric field equipotential lines between each two paired markers that possess the same symbols. The size of each square grid was 100 μm; therefore, while applying 30 V on F-MEC, the variation in gradient of electric field strength was 0.1×10^4 V/m per 100 μm. As shown in Figure 4A, by analyzing the cell viability around each equipotential line, the relationship between cell viability and electric field strength was quantitatively calculated, as shown in Figure 4B. The cell viabilities were normalized to the control group in which the same cells were incubated on another F-MEC chip, with neither bleomycin treatment nor electric stimulation. The results revealed that 2.7×10^4 V/m electric field killed ~50% of MCF-7 tumor cells while <10% cells remained viable under 3.5×10^4 V/m. Moreover, in the same assay, the cell viability for all different electric field strengths between 2.3 and 3.7×10^4 V/m could be calculated. For instance, the cell viability under 2.5×10^4 V/m was ~70%. These accurate cell viability data benefit precisely balancing the tumor suppressing and adverse effects while performing ECT.

To evaluate if F-MEC can be applied on other cell types, A-375, a human malignant melanoma cell line, was used to verify the performance of F-MEC. Malignant melanoma typically occurs in the skin and is considered as the most dangerous type of skin cancer. We used three-electrode mode and the same experimental protocol as we used in the MCF-7 assay. As shown in Figure 5, no matter if the applied voltage was 150 V or 200 V, it was clear that the cell death/survival boundary was located around 4.5×10^4 V/m. The results demonstrated that different types of tumor cells require different electric field strength to maximize the ECT effect, as well as minimize the adverse effects.

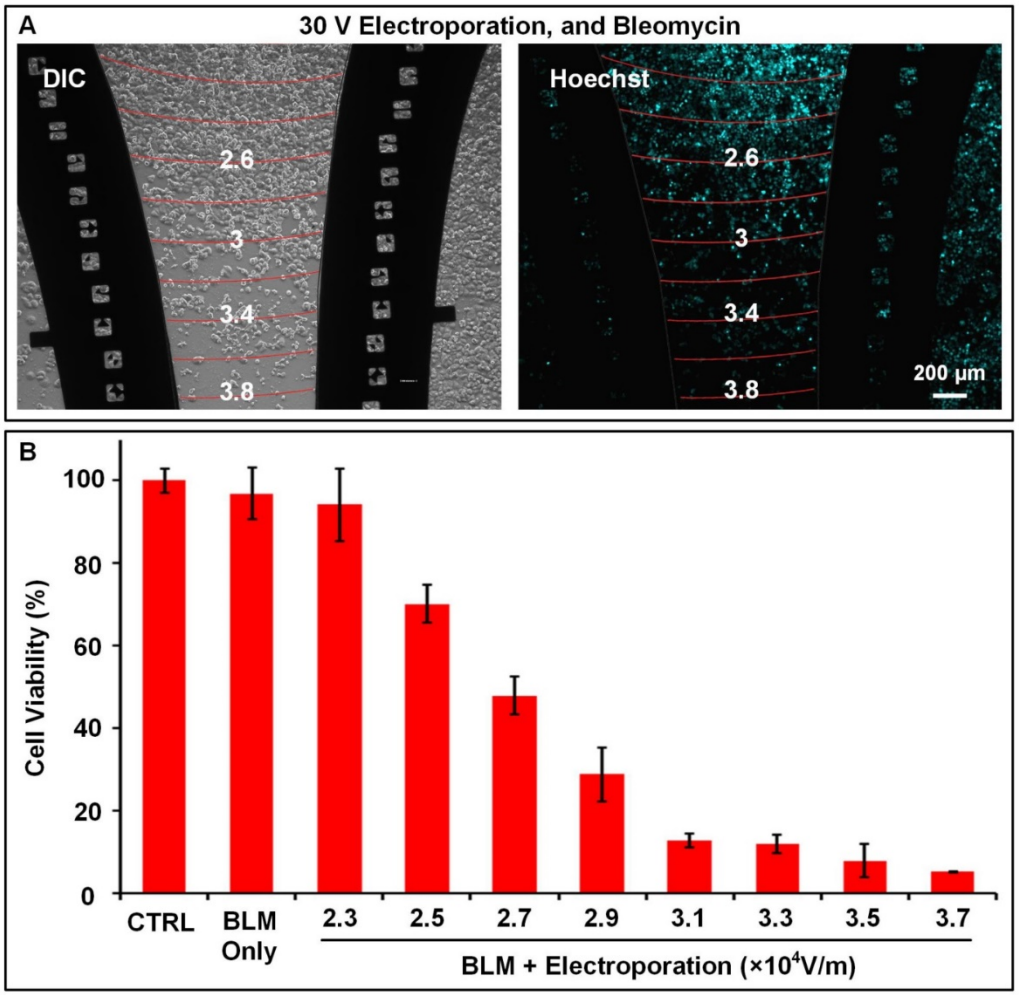

Figure 4. Quantitative analysis of the relationship between cell viabilities and electric field strengths Bright field image (A left) and fluorescence image (A right) of Hoechst stained MCF-7 cells 48 h after performing *in vitro* ECT with three-electrode stimulation mode. The conditions are: 30 V, 150 μg/mL bleomycin, 8 square electrical pulses (100 μs pulse duration and 1 s interval). The location markers fabricated in the electrodes were used to rapidly plot the electric field contours, which are labelled as red curves in (A). The Arabic numerals on the curves represent the contour values (unit: $\times 10^4$ V/m). (B) The relationship between cell viability and ECT conditions. All data are the average of three independent assays and normalized to a control group that experienced neither bleomycin nor electroporation. Each data is shown as the mean ± S.D.

The above assays were performed on cell monolayers. Considering tumors have complex structures and microenvironments, we tested cell clusters on F-MEC with the assistance of Matrigel matrix (Supplementary Figure S6). Despite this proof-of-concept assay where we simply introduced biomimetic cues from the tumor microenvironment, more complex multicellular analogs of tumors should be tested before constructing tumor models on F-MEC.

Overall, while using F-MEC to determine the optimal ECT electrical parameters for a specific tumor cell type, a relatively higher voltage, such as 150 V could be applied on F-MEC to generate a wider range of electric field strength. Thus, the suitable electric field could be rapidly determined. If a more accurate number for optimal electric field strength was required, a few more assays should be performed with a relatively lower voltage, such as 30 V, to calculate the precise relationship between cell viability and electric field strength. How we calculate the data errors decides the number of F-MEC assays that ought to be used, usually less than 3.

In vivo verification of optimized ECT parameters

After acquiring optimal ECT electrical parameters by F-MEC, we designed a tumor suppression assay in mice to verify if *in vitro* acquired parameters are applicable *in vivo*. In ECT, subcutaneous tumor is relatively difficult because the skin prevents direct contact between electrodes and target tissue. A subcutaneous MCF-7 xenografted murine tumor model was established to test the optimal parameters from *in vitro* MCF-7 assays on F-MEC. When the tumor grew to about 300 mm^3, the mice were randomly divided into 8 groups (6 mice in each group): group 1, without any treatment; group 2,

without bleomycin injection, and stimulated by 250 V; group 3, with bleomycin injection, but without electrical stimulation; group 4, 5, 6, 7 and 8, with bleomycin and electrical stimulation under 50, 100, 150, and 250 V, respectively. Electrical stimulations were applied on tumors by an electroporation clamp.

Considering the existence of high-resistance skin, the relationship between voltages applied on skin and actual electric field strengths applied on tumor tissue were calculated by FEA (finite element analysis). The detailed calculation process is described in Supplementary Figure S5. Every day for 3 days, ECT was repeated on each mouse. The tumor sizes were monitored for 17 days. As shown in Figure 6A, tumor volume in the control group grew 3.46-fold, while tumor volumes in the groups solely administered either electrical stimulation (group 2) or bleomycin (group 3) grew >3-fold, exhibiting no tumor suppression. For groups 4, 5, and 6, the applied voltages were too weak to mediate efficient ECT. For group 7, in which 200 V was applied and the corresponding effective electric field strength was ~3×10^4 V/m, the tumor volume increased only 1.27-fold. For group 8, further increasing the voltage to 250 V (effective electric field strength 3.75 $\times10^4$ V/m) brought slight improvement in tumor suppression. Apart from MCF-7 cells, we also tested the optimized electric field for ECT for A375 cells in mice. As shown in Figure 6B, the *in vitro* optimized electric field strength (4.5 $\times10^4$ V/m) was proved valid *in vivo*. The results demonstrated that the optimal electric field value acquired from *in vitro* assay fitted the *in vivo* ECT tests. Moreover, for subcutaneous xenografted murine tumor models, optimal voltages (200 V for MCF-7 cells and 300 V for A375 cells) were significantly lower than SOP recommended numbers (960 V). While applying voltages of 250 V and 300 V, slight electrical burn marks were observed on mice skins, which recovered in 48 h. While applying 400 V voltage, severe electrical burns occurred that did not recover during the whole experimental period (Supplementary Figure S6). This reveals that performing *in vitro* determination is helpful for achieving optimal balance between ECT therapeutic effects and adverse effects.

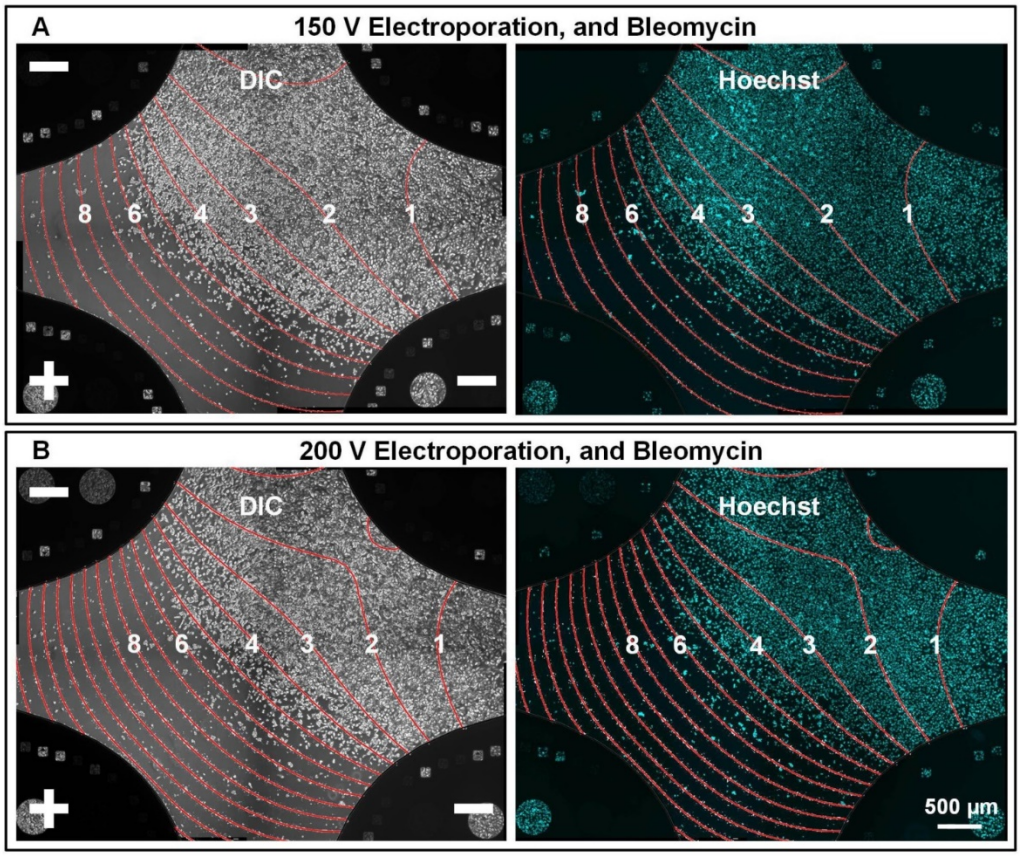

Figure 5. In situ monitoring the bleomycin responses of A-375 cells on F-MEC under three-electrode stimulation mode Bright field images (left) and fluorescence images (right) of Hoechst stained A-375 cells 48 h after performing *in vitro* ECT with three-electrode stimulation mode. The upper right electrode was disconnected from the electric stimulator. The conditions are: (A) 150 V and 150 μg/mL bleomycin; (B) 200 V and 150 μg/mL bleomycin. For both (A) and (B), 8 square electrical pulses (100 μs pulse duration and 1 s interval) were applied. In each image, the electric field contours are marked by red curves and the Arabic numerals on the curves represent the contour values (unit: $\times10^4$ V/m).

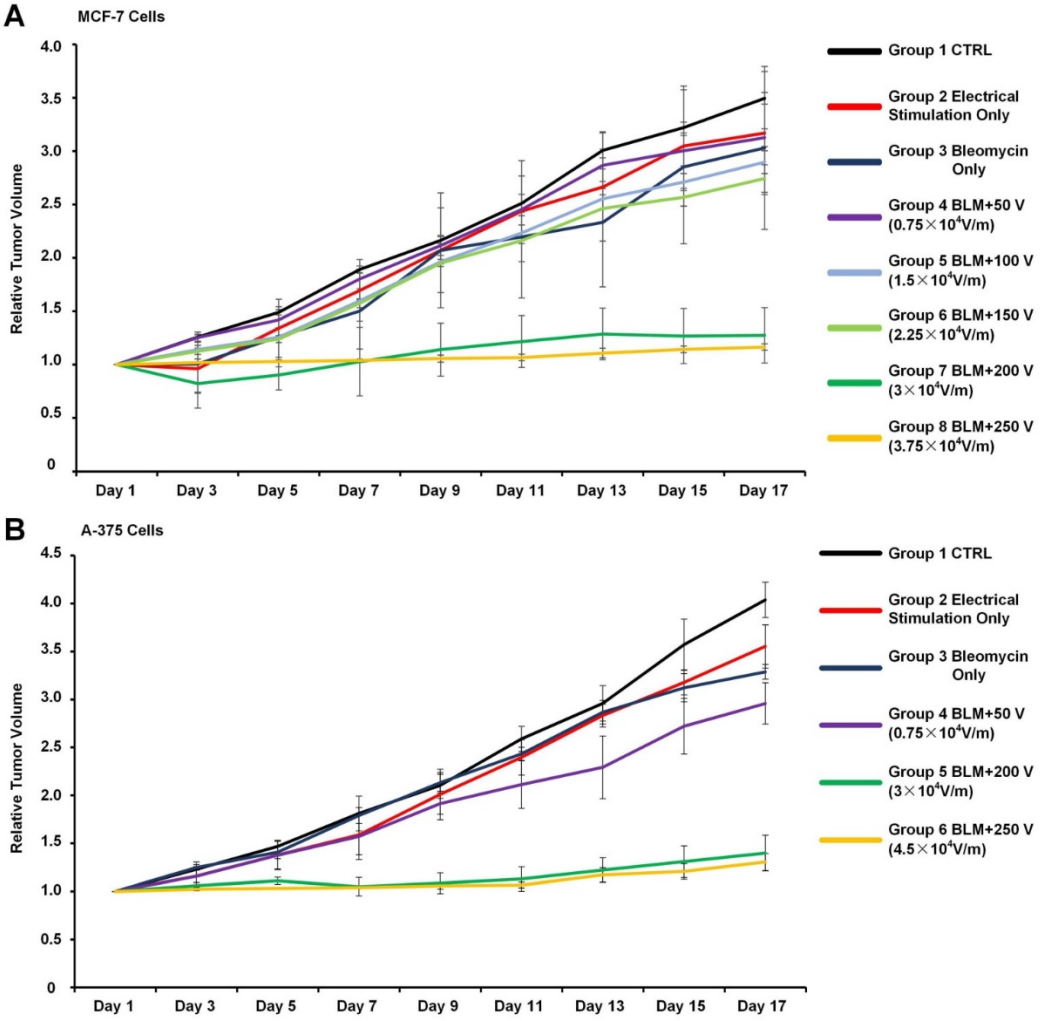

Figure 6. The relationship between tumor suppression effects and ECT parameters. (A) For MCF-7 tumors, the mice were randomly divided into 8 groups (6 mice in each group): group 1, without any treatment; group 2, without bleomycin injection and electrically stimulated by 250 V; group 3, with bleomycin injection but without electrical stimulation; group 4, 5, 6, 7 and 8, with bleomycin and electrical stimulation of 50, 100, 150, 200 and 250 V, respectively. (B) For A-375 tumors, the mice were randomly divided into 6 groups (6 mice in each group): group 1, without any treatment; group 2, without bleomycin injection and electrically stimulated by 300 V; group 3, with bleomycin injection but without electrical stimulation; group 4, 5 and 6, with bleomycin and electrical stimulation of 200, 300 and 400 V, respectively. For both (A) and (B), other ECT parameters are: 10 square electrical pulses, 1 s interval, 10 ms pulse duration. The relative tumor volume was calculated by normalizing the mean tumor volume of post-treatment mice to the corresponding mean tumor volume before treatments. Each bar represents the mean ± SD.

Discussion and Conclusion

ECT is one of the very few available treatments for cutaneous and subcutaneous tumors when surgery and radiotherapy are no longer available. Many adverse effects, including pain, bleeding, electrically burnt skin and uncontrollable muscle contraction were reported in previous clinical practices due to excessive voltages, which are recommended in existing SOP to ensure killing of tumor cells. The main reason for simply fixing a high voltage for all tumor types in the SOP was that it is impossible or clinically unacceptable to exhaust all possible voltages for diverse patients, either *in vivo* or *in vitro*.

This study provides a feasible solution by developing a F-MEC chip in which the electric field was specially designed by linear distribution to cover all possible electric field strengths for ECT. Therefore, by *in situ* monitoring the cell responses to ECT drugs, such as bleomycin, the optimal electric field strength for any given cell type could be rapidly calculated in a few, or even only one, simple assay. This chip-based parametric optimization method has the following prominent features: i) Instead of previous "trial and error" approaches, which are time-costly and only cover limited electric fields, the F-MEC provides a possibility to test all possible electric field strengths in only one assay, making cost, labor and time consumption of individual ECT become clinically acceptable. ii) Different electrical conditions are simultaneously tested in the same chip in which all cells and drugs are in the same status, minimizing experimental errors and therefore ensuring the

consistency and reliability of the test. More importantly, the *in vivo* tumor suppression assays in our study proved that the optimal parameters acquired from *in vitro* F-MEC assay could be used for *in vivo* ECT. In this proof-of-concept study, the same cell type was used in both *in vitro* determination and *in vivo* testing. Normally, surgery and/or radiotherapy are performed before ECT; therefore, it would be easy to isolate tumor cells from excised tumor tissue or biopsy samples. The isolated tumor cells from patients could be cultured on the F-MEC for *in vitro* determination, ensuring that the data acquired from *in vitro* determination are applicable for clinical ECT.

Abbreviations

ECT: electrochemotherapy; SOP: standard operating procedures; F-MEC: four-leaf micro-electrode chip; DMEM: Dulbecco's modified Eagle's medium; SPF: specific pathogen free; FEA: finite element analysis. BLM: Bleomycin.

Supplementary Material

Supplementary Figure S1: *In situ* monitoring the DNA expression on F-MEC. Supplementary Figure S2: Analyzing cell existence/survival/death. Supplementary Figure S3: *In situ* monitoring the cell apoptosis on F-MEC. Supplementary Figure S4: Cell clusters on F-MEC. Supplementary Figure S5: Calculation of electrical field distribution. Supplementary Figure S6: Skin damages. http://www.thno.org/v08p0358s1.pdf

Acknowledgements

This work was supported by the National Natural Science Foundation of China (No 81502586, 81473128 and 61204118).

Author Contribution

D. Z., M. W., Z. W., Zh. L. and Z. L. designed research. D. Z. and Z. W wrote this manuscript. M. W. and D. H., fabricated the electroporation device. M. W. and D. H. performed the F-MEC simulation. D. Z. and Z. W. coordinated animal assays. D. Z. conducted cell electroporation. D. Z., M. W., D. H. and Z. W. analyzed the transfection data and provided helpful discussion. All authors discussed results and commented on the paper.

Competing Interests

The authors have declared that no competing interest exists.

References

1. Mir LM, Glass LF, Sersa G, Teissie J, Domenge C, Miklavcic D, et al. Effective treatment of cutaneous and subcutaneous malignant tumours by electrochemotherapy. Br J Cancer. 1998; 77: 2336-42.
2. Testori A, Tosti G, Martinoli C, Spadola G, Cataldo F, Verrecchia F, et al. Electrochemotherapy for cutaneous and subcutaneous tumor lesions: a novel therapeutic approach. Dermatol Ther. 2010; 23: 651-61.
3. Madero VM, Perez GO. Electrochemotherapy for treatment of skin and soft tissue tumours. Update and definition of its role in multimodal therapy. Clin & Trans Oncology. 2011; 13: 18-24.
4. Groselj A, Kos B, Cemazar M, Urbancic J, Kragelj G, Bosnjak M, et al. Coupling treatment planning with navigation system: a new technological approach in treatment of head and neck tumors by electrochemotherapy. Biomed Eng Online. 2015; 14: 14.
5. Kodre V, Cemazar M, Pecar J, Sersa G, Cor A, Tozon N. Electrochemotherapy compared to surgery for treatment of canine mast cell tumours. In Vivo. 2009; 23: 55-62.
6. Lowe R, Gavazza A, Impellizeri JA, Soden DM, Lubas G. The treatment of canine mast cell tumours with electrochemotherapy with or without surgical excision. Vet Comp Oncol. 2016.
7. Campana LG, Bertino G, Rossi CR, Occhini A, Rossi M, Valpione S, et al. The value of electrochemotherapy in the treatment of peristomal tumors. Ejso-Eur J Surg Onc. 2014; 40: 260-2.
8. Sersa G, Grp E. Electrochemotherapy in treatment of solid tumours in cancer patients. Ifmbe Proc. 2007; 16: 614-7.
9. Tarantino L, Busto G, Nasto A, Fristachi R, Cacace L, Talamo M, et al. Percutaneous electrochemotherapy in the treatment of portal vein tumor thrombosis at hepatic hilum in patients with hepatocellular carcinoma in cirrhosis: A feasibility study. World J Gastroentero. 2017; 23: 906-18.
10. Jahangeer S, Forde P, Soden D, Hinchion J. Review of current thermal ablation treatment for lung cancer and the potential of electrochemotherapy as a means for treatment of lung tumours. Cancer Treat Rev. 2013; 39: 862-71.
11. Munoz Madero V, Ortega Perez G. Electrochemotherapy for treatment of skin and soft tissue tumours. Update and definition of its role in multimodal therapy. Clin Transl Oncol. 2011; 13: 18-24.
12. Jahangeer S, Forde P, Soden D, Hinchion J. Pre-Clinical Validation of Electrochemotherapy (Ect) in the Treatment of Lung Tumours. J Thorac Oncol. 2013; 8: S463-S.
13. Testori A, Pennacchioli E, Ferrucci PF, Tosti G, Verrecchia F, Cocorocchio E, et al. Electrochemotherapy: A treatment with specific intent in specific skin tumors-Experience Front the European institute of Oncology, Milan. J Clin Oncol. 2014; 32.
14. Orlowski S, Belehradek J, Jr., Paoletti C, Mir LM. Transient electropermeabilization of cells in culture. Increase of the cytotoxicity of anticancer drugs. Biochem Pharmacol. 1988; 37: 4727-33.
15. Cemazar M, Tamzali Y, Sersa G, Tozon N, Mir LM, Miklavcic D, et al. Electrochemotherapy in veterinary oncology. J Vet Intern Med. 2008; 22: 826-31.
16. Mir LM, Gehl J, Sersa G, Collins CG, Garbay JR, Billard V, et al. Standard operating procedures of the electrochemotherapy: Instructions for the use of bleomycin or cisplatin administered either systemically or locally and electric pulses delivered by the Cliniporator (TM) by means of invasive or non-invasive electrodes. Ejc Suppl. 2006; 4: 14-25.
17. Testori A, Soteldo J, Powell B, Sales F, Borgognoni L, Rutkowski P, et al. Surgical management of melanoma: an EORTC Melanoma Group survey. Ecancer. 2013; 7: 294-308.
18. Miklavcic D, Sersa G, Brecelj E, Gehl J, Soden D, Bianchi G, et al. Electrochemotherapy: technological advancements for efficient electroporation-based treatment of internal tumors. Med Biol Eng Comput. 2012; 50: 1213-25.
19. Calmels L, Al-Sakere B, Ruaud JP, Leroy-Willig A, Mir LM. In vivo MRI Follow-up of Murine Tumors Treated by Electrochemotherapy and other Electroporation-based Treatments. Technol Cancer Res T. 2012; 11: 561-70.
20. Byrne CM, Thompson JF. Role of electrochemotherapy in the treatment of metastatic melanoma and other metastatic and primary skin tumors. Expert Rev Anticanc. 2006; 6: 671-8.
21. Cemazar M, Sersa G, Miklavcic D. Electrochemotherapy with cisplatin in the treatment of tumor cells resistant to cisplatin. Anticancer Res. 1998; 18: 4463-6.
22. Spugnini EP, Baldi F, Mellone P, Feroce F, D'Avino A, Bonetto F, et al. Patterns of tumor response in canine and feline cancer patients treated with electrochemotherapy: preclinical data for the standardization of this treatment in pets and humans. J Transl Med. 2007; 5: 48-53.
23. Spugnini EP, Vincenzi B, Citro G, Dotsinsky I, Mudrov T, Baldi A. Evaluation of Cisplatin as an Electrochemotherapy Agent for the Treatment of Incompletely Excised Mast Cell Tumors in Dogs. J Vet Intern Med. 2011; 25: 407-11.
24. Weaver JC. Electroporation of biological membranes from multicellular to nano scales. Ieee T Dielect El In. 2003; 10: 754-68.
25. Neumann E, Schaeferridder M, Wang Y, Hofschneider PH. Gene-Transfer into Mouse Lyoma Cells by Electroporation in High Electric-Fields. Embo J. 1982; 1: 841-5.
26. Tounekti O, Kenani A, Foray N, Orlowski S, Mir LM. The ratio of single- to double-strand DNA breaks and their absolute values determine cell death pathway. Br J Cancer. 2001; 84: 1272-9.

27. Miklavcic D, Mali B, Kos B, Heller R, Sersa G. Electrochemotherapy: from the drawing board into medical practice. Biomed Eng Online. 2014; 13: 29-48.
28. Breton M, Mir LM. Microsecond and nanosecond electric pulses in cancer treatments. Bioelectromagnetics. 2012; 33: 106-23.
29. Larkin JO, Casey GD, Tangney M, Cashman J, Collins CG, Soden DM, et al. Effective tumor treatment using optimized ultrasound-mediated delivery of bleomycin. Ultrasound Med Biol. 2008; 34: 406-13.
30. Larkin JO, Collins CG, Aarons S, Tangney M, Whelan M, O'Reily S, et al. Electrochemotherapy: aspects of preclinical development and early clinical experience. Ann Surg. 2007; 245: 469-79.
31. Miklavcic D, Semrov D, Mekid H, Mir LM. A validated model of in vivo electric field distribution in tissues for electrochemotherapy and for DNA electrotransfer for gene therapy. Biochim Biophys Acta. 2000; 1523: 73-83.
32. Sersa G, Miklavcic D, Cemazar M, Rudolf Z, Pucihar G, Snoj M. Electrochemotherapy in treatment of tumours. Eur J Surg Oncol. 2008; 34: 232-40.
33. Soden DM, Larkin JO, Collins CG, Tangney M, Aarons S, Piggott J, et al. Successful application of targeted electrochemotherapy using novel flexible electrodes and low dose bleomycin to solid tumours. Cancer Lett. 2006; 232: 300-10.
34. Gothelf A, Mir LM, Gehl J. Electrochemotherapy: results of cancer treatment using enhanced delivery of bleomycin by electroporation. Cancer Treat Rev. 2003; 29: 371-87.
35. Spugnini EP, Renaud SM, Buglioni S, Carocci F, Dragonetti E, Murace R, et al. Electrochemotherapy with cisplatin enhances local control after surgical ablation of fibrosarcoma in cats: an approach to improve the therapeutic index of highly toxic chemotherapy drugs. J Transl Med. 2011; 9: 152-6.
36. Marty M, Sersa G, Garbay JR, Gehl J, Collins CG, Snoj M, et al. Electrochemotherapy - An easy, highly effective and safe treatment of cutaneous and subcutaneous metastases: Results of ESOPE (European Standard Operating Procedures of Electrochemotherapy) study. Ejc Suppl. 2006; 4: 3-13.
37. Girelli R, Prejano S, Cataldo I, Corbo V, Martini L, Scarpa A, et al. Feasibility and safety of electrochemotherapy (ECT) in the pancreas: a pre-clinical investigation. Radiol Oncol. 2015; 49: 147-54.
38. Gallego-Perez D, Chang L, Shi J, Ma J, Kim SH, Zhao X, et al. On-Chip Clonal Analysis of Glioma-Stem-Cell Motility and Therapy Resistance. Nano Lett. 2016; 16: 5326-32.
39. Bao N, Le TT, Cheng JX, Lu C. Microfluidic electroporation of tumor and blood cells: observation of nucleus expansion and implications on selective analysis and purging of circulating tumor cells. Integr Biol (Camb). 2010; 2: 113-20.
40. Choi YS, Kim HB, Kwon GS, Park JK. On-chip testing device for electrochemotherapeutic effects on human breast cells. Biomed Microdevices. 2009; 11: 151-9.
41. Choi YS, Kim HB, Kim SH, Choi J, Park JK. Microdevice for analyzing the effect of electrochemotherapy on cancer cells. Anal Chem. 2009; 81: 3517-22.